TÜBİTAK

Turkish Journal of Earth Sciences

http://journals.tubitak.gov.tr/earth/

Research Article

Turkish J Earth Sci
(2018) 27: 32-48

doi:10.3906/yer-1705-21

Reconstructing the sedimentary evolution of the Miocene Aksu Basin based on fan delta development (eastern Mediterranean-Turkey)

Serkan ÜNER[1,*], Erman ÖZSAYIN[2], Ramazan Kadir DİRİK[2], Tahsin Attila ÇİNER[3], Mustafa KARABIYIKOĞLU[4]

[1]Department of Geological Engineering, Faculty of Engineering, Van Yüzüncü Yıl University, Van, Turkey
[2]Department of Geological Engineering, Faculty of Engineering, Hacettepe University, Ankara, Turkey
[3]Eurasia Institute of Earth Sciences, İstanbul Technical University, İstanbul, Turkey
[4]Department of Geography, Ardahan University, Ardahan, Turkey

Received: 25.05.2017 • **Accepted/Published Online:** 21.11.2017 • **Final Version:** 08.01.2018

Abstract: The Aksu Basin in southern Turkey is dominantly represented by an alluvial fan and five fan deltas (FDs) developed along the tectonically controlled margins of the basin during the Miocene. Four alternating compressional and tensional tectonic phases have influenced the basin since its formation. Strong tectonic movements caused high sedimentation rates and progradation of large debris-flow and mass-flow dominated FDs. Here we describe two FDs (the Karadağ and Kargı FDs) in detail. The Karadağ FD began to develop under the control of a compressional regime and continued the evolution under a tensional regime. The same tensional regime caused the separation of the Karadağ FD from its source and the deposition of the Kargı FD into the newly formed accommodation area. The alternating tectonic regimes and sea-level oscillations in the Aksu Basin gave rise to the development of coral colonies on the shallow delta fronts, forming patch reefs despite the large amounts of conglomerates supplied by fan deltaic processes.

Key words: Fan delta, sedimentary facies, sedimentary evolution, Aksu Basin, eastern Mediterranean

1. Introduction

Fan deltas (FDs) are gravel-rich deltas formed where an alluvial fan is deposited directly into a standing body of water from an adjacent highland (McPerson et al., 1987). Their subaerial components correspond to steep alluvial fans that are mainly composed of interbedded sheetflood, debris-flow, and braided-channel deposits (Nemec and Steel, 1988). FDs often show changing paleocurrent directions and abrupt facies changes in the geological record. Their deposits are often very coarse-grained (with occasional large boulders) and very poorly sorted, and reef bodies might develop in their subaqueous parts (Tucker and Wright, 1990).

Several alluvial fan and FD sequences originating from the southern Tauride Mountain Range have been previously described in Turkey. Examples from the Kasaba Basin (Hayward and Robertson, 1982) and Çatallar Basin (Koşun et al., 2009) from the southwestern Taurides are well known. Other important alluvial fan-FD complexes are observed in the Miocene Antalya Basins (Flecker et al., 1998; Glover and Robertson, 1998a, 1998b; Deynoux et al., 2005; Çiner et al., 2008; Poisson et al., 2011). For instance, Karabıyıkoğlu et al. (2000) described thick alluvial fans in the Miocene Manavgat Basin. In the Köprüçay Basin, adjacent to the Aksu Basin of the present study, Deynoux et al. (2005) also described three distinct alluvial fan-FD systems with extensive conglomeratic successions and patch reefs that pass laterally into pelagic mudstones towards the deeper parts of the basin.

The Aksu Basin, the subject of this study, experienced multistage tectonism (Flecker et al., 1998; Glover and Robertson, 1998b; Poisson et al., 2011; Üner et al., 2015; Koç et al., 2016) and that activity led to the formation of alluvial fan/FD bodies at the basin. An alluvial fan (Eskiköy) and five FD sequences (Kapıkaya, Kozan, Karadağ, Kargı, and Bucak FDs) play a major role in the sedimentary evolution of the basin. The Eskiköy alluvial fan and Kapıkaya, Kozan, and Bucak FDs completed their evolutions under a single extensional regime, but the Karadağ and Kargı FDs were affected by all the phases that the Aksu Basin has witnessed and constitute the main focus of our study.

The aim of this study is to determine the sedimentological evolution of the Aksu Basin under the influence of structural instability by the help of FD deposits, which are widespread during and after Miocene

* Correspondence: suner@yyu.edu.tr

times. Stratigraphic, sedimentological, and structural characteristics of the FDs are evaluated together and an evolutionary model of the basin since the Langhian is suggested within the scope of the study.

2. Geological setting

The study area is located within the Isparta Angle, which is one of the most important morphotectonic features exposed in southwestern Anatolia. This inverse V-shaped structure to the north of Antalya Bay in southern Turkey, where the Aegean and Cyprian Arcs intersect in the eastern Mediterranean, was first described by Blumenthal (1951) (Figure 1a). The Isparta Angle is kinematically linked to the West Anatolian Extensional Province by the NE-striking Fethiye-Burdur Fault Zone to the west (Barka et al., 1997) and the Anatolian Plateau by the NW-striking Akşehir Fault Zone to the east (Koçyiğit and Özacar, 2003; Özsayın and Dirik, 2007, 2011; Özsayın et al., 2013). It constitutes the transition between the uplifting (Schildgen et al., 2012; Çiner et al., 2015) and westward moving Anatolian Plateau and southwestward displacing and counter-clockwise rotating West Anatolian province.

The Antalya Basin, located within the Isparta Angle, has been developing unconformably over the Antalya, Beyşehir-Hoyran-Hadım, and Lycian Nappe sheets since the Late Cenozoic. In present day plan-view, this basin consists of three subbasins, namely the Aksu, Köprüçay, and Manavgat Basins. The N-S striking Kırkkavak Fault and W- to SW-verging Aksu Thrust are the two major structures dividing these three basins (Dumont and Kerey, 1975; Akay et al., 1985; Monod et al., 2006; Çiner et al., 2008; Poisson et al., 2011; Hall et al., 2014) (Figure 1b).

The Aksu Basin experienced 4 stages in its structural evolution (Üner et al., 2015). The first phase is the NW-SE-oriented contraction caused by the emplacement of the Lycian Nappes, which ended in the Langhian. This phase, which induced the formation and the initial deformation of the basin, is followed by a NW-SE tensional stress regime. The regime prevailed between the Langhian and Messinian and was terminated by a NE-SW compressional stress regime known as the Aksu Phase. The neotectonic period is characterized by NE-SW extension initiated in the Late Pliocene (Üner et al., 2015).

3. Methods

In order to determine the tectonosedimentary evolution of the Karadağ and Kargı FDs in time and space, we clarified the boundary relationship between basement rocks and basin infill of the basin and revised the 1:100,000 scale geological maps of the Mineral Research and Exploration Institute of Turkey (Turkish abbreviation: MTA) (Figure 2a). Bedding plane measurements were taken from basin fill to control the tectonic and sedimentological interpretation and two sedimentary logs were taken from FDs to define sedimentary facies and analyze the sedimentary environment changes. Fifteen facies are partially adopted from previous studies (e.g., Karabıyıkoğlu et al., 2004; Çiner et al., 2008; Üner, 2009) and used to

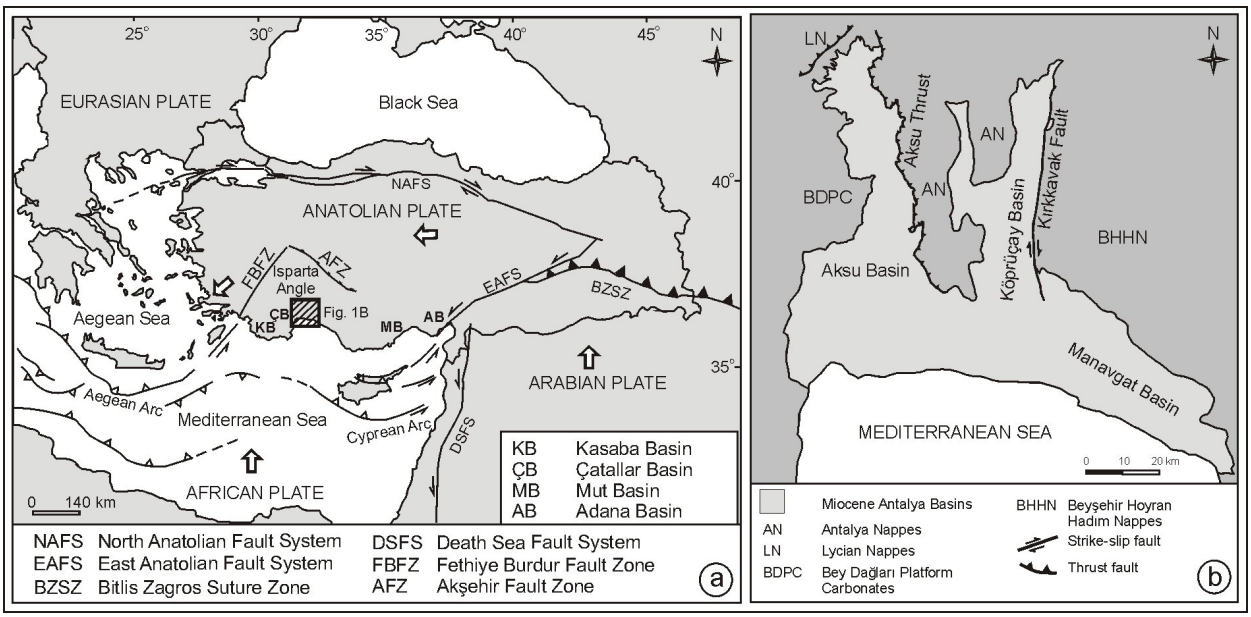

Figure 1. a) Major neotectonic features of Turkey and adjacent areas (compiled from Koçyiğit and Özacar, 2003; Zitter et al., 2003; Özsayın, 2007; Üner et al., 2015) (white arrows indicate the motion of the plates). b) Location and boundaries of Aksu, Köprüçay, and Manavgat basins in the Isparta Angle.

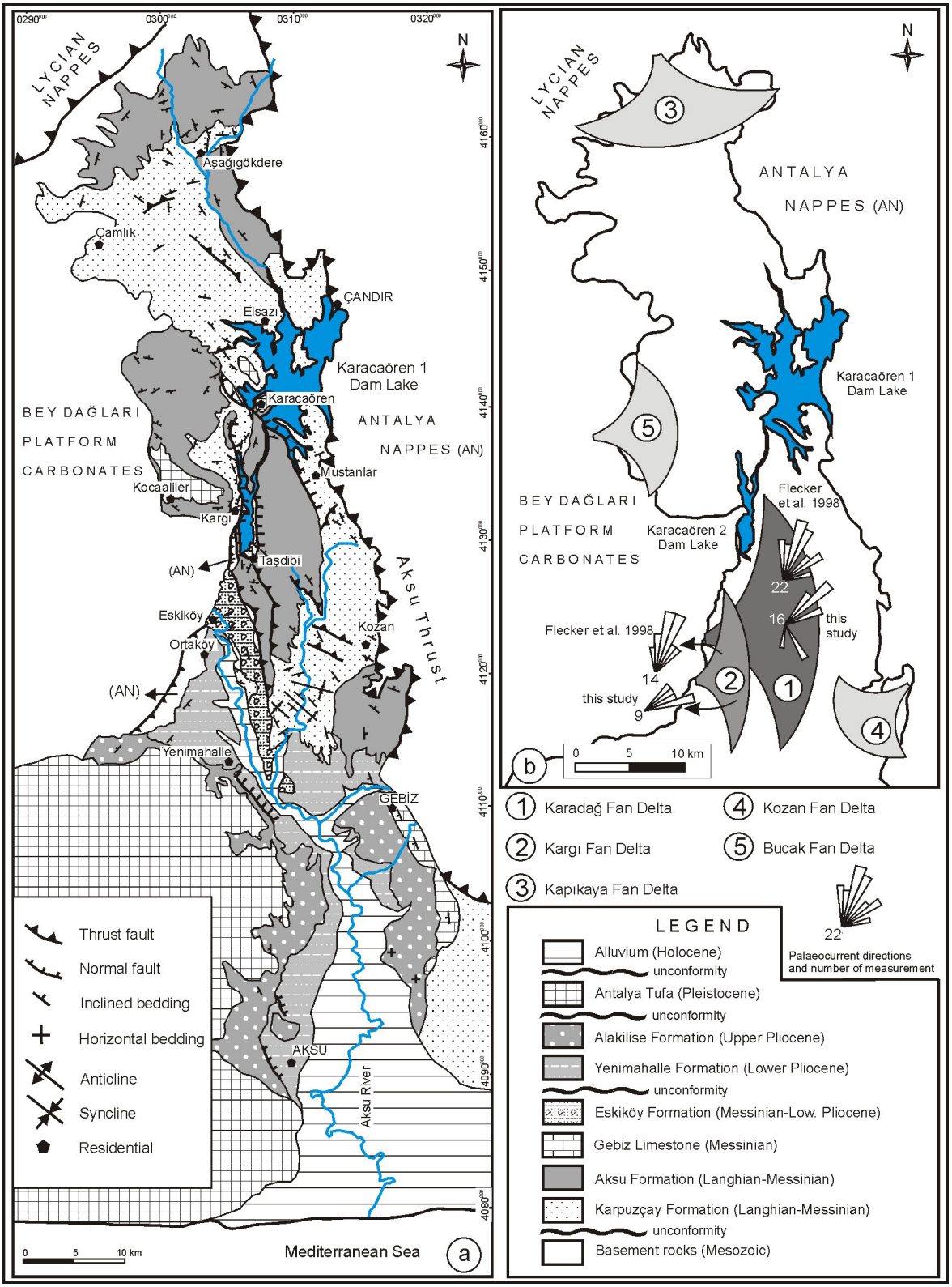

Figure 2. a) Geological map of the Aksu Basin (modified from Akay and Uysal, 1984; Şenel, 1997; Glover and Robertson, 1998a; Karabıyıkoğlu et al., 2004; Monod et al., 2006; Üner, 2009; Poisson et al., 2011). b) Location of the FDs in Aksu Basin.

explain the depositional environments. Paleocurrent data from imbrications of pebbles, flute casts, cross-bedding, and current ripple marks were collected and combined with previous studies (Figure 2b).

4. Stratigraphy

The N-S trending Aksu Basin covers approximately 2000 km^2 and is bounded by the Bey Dağları Platform Carbonates to the west and by the Aksu Thrust to the east within the central part of the Isparta Angle (Figure 2a). The basin fill starts with the Langhian-Tortonian Karpuzçay Formation (Akay et al., 1985; Karabıyıkoğlu et al., 2004), which is composed of shallow marine conglomerates intercalating with sandstone-mudstone alternations. It unconformably overlies the basement units consisting of Bey Dağları Platform Carbonates, Alanya Metamorphics, and Antalya Nappes (ophiolite) and Lycian Nappes (platform carbonate). The Langhian-Messinian Aksu Formation interfingers with the Karpuzçay Formation (Karabıyıkoğlu et al., 2004) and is composed of five different FDs that are fed from the north (Kapıkaya FD), west (Karadağ, Kargı and Bucak FDs), and east (Kozan FD) of the basin (Figure 2b). Thick-bedded, consolidated conglomerates of the Aksu Formation, together with patch reefs (Karabıyıkoğlu et al., 2005) and intercalated sandstones-marls, gradually pass to Messinian Gebiz Limestones (Çiner et al., 2008) and the Messinian-Pliocene Eskiköy Formation (Şenel, 1997). The Eskiköy Formation is represented by alluvial fan and fluvial deposits and is composed of poorly consolidated conglomerates, sandstones, and marls (Figure 3).

The transition from shallow marine to terrestrial environments in the basin took place during the Messinian Salinity Crisis. Because of the rising sea level following the salinity crisis, marine conditions prevailed in the southern part of the Aksu Basin, whereas northern parts remained terrestrial. The Eskiköy Formation is unconformably overlain by the shallow marine (marl-sandstone) Yenimahalle Formation during that period (Poisson et al., 2003). These units grade from lacustrine to a fluvial Pliocene Alakilise Formation made up of thick-bedded conglomerates, lacustrine limestones, and siltstones (Poisson et al., 2003). The uppermost part of the basin fill is composed of Quaternary Antalya tufa and alluvium (Koşun, 2012) (Figure 3).

5. Sedimentology

5.1. Sedimentary facies

The Miocene fill of the Aksu Basin is mainly characterized by continental to shallow marine coarse clastic rocks originating from the several alluvial fans and FDs mentioned above. Using facies previously described by the authors (Karabıyıkoğlu et al., 2004; Çiner et al., 2008; Üner, 2009), we grouped the Karadağ and Kargı FD sediments into fifteen facies (Table). These are (a) limestone breccia (F1), (b) matrix-supported conglomerate (F2), (c) clast-supported conglomerate (F3), (d) large-scale cross-stratified conglomerate (F4), (e) parallel-stratified conglomerate (F5), (f) graded conglomerate (F6), (g) massive to parallel-stratified gravelly sandstone (F7), (h) cross-stratified conglomerate and sandstone (F8), (j) normally graded sandstone (F9), (k) massive pebbly mudstone (F10), (m) graded siltstone and mudstone (F11), (n) massive to parallel laminated siltstone-mudstone (F12), (p) chaotically folded deposits (F13), (q) reefal debrites (F14), and (r) massive coral-algal boundstone (F15) (Figure 4).

6. Description of fan deltas

6.1. Karadağ fan delta

Serravalian-Tortonian FD deposits composed of sandstones and gravels of limestones and ophiolitic rocks, which are located at the central part of the Aksu Basin, are named as Karadağ Conglomerates (Karabıyıkoğlu et al., 2004). This unit has approximately 750 m thickness and is composed of NE-dipping thick-bedded (30–100 cm) conglomerates. The gravels of this unit are medium to poorly sorted, semirounded/rounded, having a size range between 3 and 8 cm with a maximum of 50 cm, and bounded by a granule/coarse sand matrix.

The thick succession of Karadağ FD deposits exposed in the central area is mainly composed of polymictic, thickly bedded subaqueous debris flows (F1, F2, F3, F6, and F8) with rare sandstone beds (F5, F7, F9, F11, and F13) and marl intercalations at the top (F10) (Figure 5a). Imbricated pebbles are very rare, as well as oblique stratifications. Reworked materials include mainly white and gray Mesozoic limestones, dark sandstones, red and green radiolarites, and ophiolitic pebbles. Although the base of the Karadağ FD is not observed due to tectonism, the facies characteristics indicate alluvial fan-FD environments. FD deposits show repetition of similar facies (Fig 5a) caused by gradual subsidence of the basin floor. This subsidence can be determined by inclination decrease of the bedding plane (Figure 5b).

Field observations and paleontological studies clearly indicate that the sources of the Karadağ FD deposits are the Bey Dağları Platform Carbonates and overthrusting Antalya Nappe units (limestones and serpentinites). Upper Cretaceous *Globotruncana* observed in Miocene Karadağ FD sediments prove the source of sediments (Figure 5c). NE- and SE-oriented paleocurrents determined from imbrication of pebbles, cross-bedding, and flute casts, which are observed within the conglomerates and sandstones, indicate the growing direction of the Karadağ FD. Paleocurrent directions obtained in this study are similar to those published by Flecker et al. (1998) (Figure 2b).

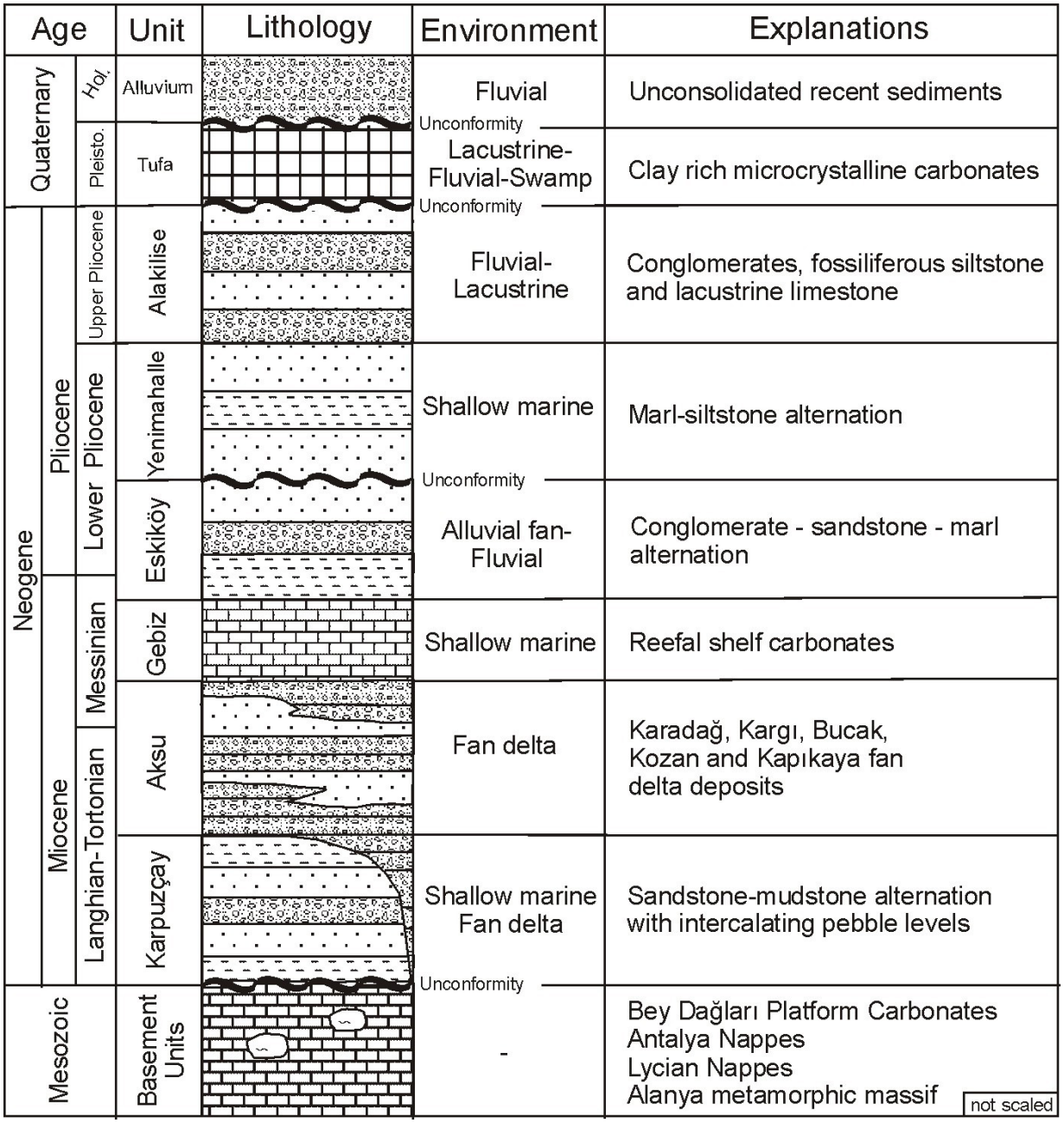

Figure 3. Stratigraphic columnar section of the study area (modified from Poisson et al., 2003, 2011; Karabıyıkoğlu et al., 2004; Üner, 2009).

6.2. Kargı fan delta

The approximately N-S trending Kargı FD is located at the western part of the Aksu Basin and composed of NE-dipping thick conglomerates intercalated with thin mudstones with a total thickness of 185 m (Karabıyıkoğlu et al., 2004; Üner et al., 2011). This unit is composed of medium to poorly sorted semirounded limestone and ophiolite-originated pebbles having gravel size between 3 and 5 cm with a maximum of 40 cm and is bounded by a granule/coarse sandy matrix. Kargı FD deposits contain well-preserved patch-reefs, which have been described in detail (Tuzcu and Karabıyıkoğlu, 2001; Flecker et al., 2005; Karabıyıkoğlu et al., 2005). The corals are mostly *Porites* and *Tarbellastraea* (including *T. siciliae*), and the age of the reefs is attributed to the Tortonian.

The lower Kargı FD deposits are characterized by a succession of matrix to clast-supported lenticular conglomerates (F1 and F2) with red mudstone (F11)

Table. Lithofacies and depositional conditions of facies of the Karadağ and Kargı FDs (modified from Karabıyıkoğlu et al., 2004; Çiner et al., 2008; Üner, 2009).

Facies	Description	Interpretation
F1: Limestone breccia	Matrix to clast-supported breccia consisting of fine to coarse-grained, poorly sorted, very angular to subrounded extraclast limestone (Figure 4a). Thin- to very thick-bedded (3–200 cm) tabular units with sharply defined flat bases and tops; occasional normal grading with red mud or carbonate matrix. Shallow marine fauna comprising mixed benthic foraminifers, coralline algae and molluscan bioclasts, pelloids, minor coral fragments echinoid plaques, and spines. Locally intercalated with conglomerates and pebbly sandstones.	Red matrix-supported breccias represent a terrestrial origin, whereas the breccias with the fossiliferous carbonate matrix indicate deposition in a shoreline environment resulting from reworked coastal colluvium/screes (Blirka and Nemec, 1998).
F2: Matrix-supported conglomerate	The facies is composed of thick-bedded (30–100 cm), very poorly sorted, subangular to rounded pebble-boulder conglomerate (Figure 4b); reddish or grayish muddy matrix with varying mixtures of granule to clay-sized material; disorganized gravel fabric with floating/protruding clasts at the top; amalgamated tabular and lenticular units with sharply to faintly defined flat bounding surfaces; occasional scoured bases.	Gravity-induced subaerial and/or subaqueous mass flow deposits from high-viscosity flows (cohesive debris flows) (Middleton and Hampton, 1976).
F3: Clast-supported conglomerate	Characterized by poorly to moderately sorted, thin to very thick amalgamated beds (3–200 cm) with subrounded to rounded pebble-boulder conglomerate (Figure 4c). Disorganized gravel fabric with occasional weak imbrication in places; tabular, lenticular or channel-fill geometry with sharply defined, flat to erosional bounding surfaces; open or closed framework with red to gray muddy, sandy or granular matrix; occasional coral fragments and disarticulated bivalves.	Subaerial to subaqueous hyperconcentrated flows such as cohesive debris flows and/or tractive stream flows (Middleton and Hampton, 1976). Deposition in alluvial fan/subaerial FD environments as longitudinal bars.
F4: Large-scale cross-stratified conglomerate	This facies is characterized by large-scale inclined conglomerate beds. Pebble-cobble conglomerate comprising sigmoidal to oblique parallel foresets (up to 3 m high clinoforms) with fine to coarse intergranular sandy matrix. Texturally polymodal, moderate to well sorted, sub- to well-rounded clasts showing parallel orientation to the bedding plane mostly with imbrications (Figure 4d).	Unidirectional subaqueous flows and/or avalanches; FD/Gilbert-type delta foresets (Postma et al, 1988)
F5: Parallel stratified conglomerate	Laterally continuous thick tabular pebble-cobble conglomerate beds (0.5–3 m thick) with sharp and flat bases and tops (Figure 4e); horizontal to subhorizontal parallel beds characterized by moderately to well-sorted, clast-supported, well-segregated, subrounded to very well rounded pebbles with calcarenitic intergranular matrix.	Laminar flows with tractive bed load in a wave modified FD front; wave reworking might have also been responsible for the development of gravel segregation locally (Orton, 1988).
F6: Graded conglomerate	Normally and inversely graded conglomerate, pebbly sandstone, and sandstone. Tabular to lenticular beds (1 to 4 m thick) with sharp or erosive bases and flat tops; occasional rip-up mud clasts, flute and groove casts, burrows and mixed shallow and deeper marine fauna (Figure 4f). Well-developed and normally graded conglomeratic beds with massive basal parts grading upwards into pebbly sandstone/sandstone; inversely graded conglomerates are clast- to matrix-supported with muddy to sandy matrix.	Gravelly high- or low-density turbidity currents (Bouma, 1962); the inverse grading is the result of turbulent and intense grain interaction or debris flow.
F7: Massive to parallel stratified gravelly sandstone	Fine to coarse-grained sandstone/gravelly sandstone composed of massive to parallel laminated single or amalgamated beds. Thin- to thick-bedded (3-100 cm), well-defined tabular units with sharp flat bases and tops; erosive-based sandstone interbeds. Asymmetrical to symmetrical ripples, well-developed bioturbation, plant debris, bivalves, coral fragments, and benthic foraminifers (Figure 4g).	Erosive base, ripples, plant debris, and coral fragments resulted from high- or low-density turbidity currents and/or sandy debris flow/grain flow (Lowe, 1982).
F8: Cross-stratified conglomerate and sandstone	Generally composed of low and high angle tabular-planar and trough cross-stratified, fine to coarse, moderately well-sorted sandstone, pebbly sandstone and pebble conglomerate with thin parallel foreset beds; occasional wave-rippled and cross-stratified sandstone up to 30 cm thick (Figure 4h).	Low-angle inclined beds imply deposition by swash-back swash processes (Massari and Parea, 1988); high-angle tabular to trough cross-stratified beds are formed by wave-originated unidirectional currents in the shoreface.

Table. (Continued).

F9: Normal graded sandstone	Typical normal grading with Bouma divisions of Ta and Tb, and/or with frequent development of Tc and Td (a complete Bouma sequence (Ta–Te) is rare). Pebbly sandstone and very coarse to fine sandstone with bed thickness between 30 and 50 cm and up to 1 m. Flat to irregular bases with decimetric scours; long flute a few centimeters long and groove casts at the base of some of the beds; planar to wavy bed tops; common vertical and horizontal burrows. Extrabasinal and/or intrabasinal clastics including well-rounded bioclastic fragments of calcareous algae, foraminifers, bivalves, and corals (Figure 4j).	Rapid deposition from highly concentrated turbidity currents, followed by deposition from suspension fall-out during normal quiet-water conditions after the density flow event (Bouma, 1962).
F10: Massive pebbly mudstone	The facies is characterized by thick (1 to 5 m), laterally continuous (several hundreds of meters) tabular beds consisting of poorly sorted pebbly mudstone with sharp to erosive bases and irregular tops (Figure 4k); angular to well-rounded clasts and rip-up mudstones randomly floating in the clay-rich muddy matrix; shelf-derived mixed fauna (benthic and planktic foraminifers and coral-algal fragments).	Cohesive subaqueous muddy debris flows (Pickering et al., 1986); rip-up mudstone clasts imply erosion of the lower muddy beds; the mixed fauna indicate reworking.
F11: Graded siltstone and mudstone	It is composed of thin- to thick-bedded (3-100 cm), laterally continuous siltstone/mudstone alternation; sharply defined flat bases and tops; locally organic-rich material, bioturbation, starved ripples, wavy bedding, and obscure varve-like normal grading from silty mudstone to mudstone (Figure 4m).	Low-density turbidity currents (Pickering et al., 1986), suspension fall out in pro-delta to shallow shelf.
F12: Massive to parallel laminated siltstone-mudstone	This facies is represented by green to dark gray parallel laminated, tabular to lenticular beds alternating with fine sandstone/siltstone including rare asymmetrical ripples. Laterally extensive, thinly interbedded (1 to 10 cm) gray siltstone and mudstone with variable carbonate content; sharply defined bases and tops. Shelf derived mixed fauna and/or in situ planktic foraminifers (Figure 4n).	Sedimentation in a relatively deep open shelf from suspension fall-out and/or low-density turbidity currents (Bouma, 1962).
F13: Chaotically folded and brecciated deposits	Thick chaotic mixture of coherently folded and contorted sandstone-siltstone and mudstone beds (3–100 cm) (Figure 4p); brecciated and balled strata and rip-up clasts randomly floating in a muddy matrix or concentrated at the upper levels of the beds. Overlying and underlying deposits are generally parallel stratified with occasional channel fills.	Slump or slide generated hydroplastic deformation and/or debris flows (Pickering et al., 1986); brecciated clasts indicate erosion of the underlying beds and considerable internal deformation.
F14: Reefal debrites and isolated blocks	Fine- to very coarse-grained, angular to rounded, clast- and/or matrix-supported reefal debrites with occasional isolated and outsized blocks embedded in a very fine-grained and parallel-stratified deposit; thin to very thick beds (3–200 cm) with flat to scoured bases and flat tops; massive to normal graded (Figure 4q).	Reef flanks; fault-generated, reefal shelf-derived debrites, olistoliths, and calciturbidites (Cook and Mullins, 1983); outsized blocks represent rock falls recognized by the underlying deformed beds or rock slides (Pickering et al., 1986).
F15: Massive coral-algal boundstone	Small, isolated, massive mound-like limestone bodies made up of in situ coralgal framework (Figure 4r) consisting of high- to low-diversity hermatypic coral colonies (mainly *Tarbellastraea*, *Porites*). Sediments filling the spaces between the frame-builders locally vary from clayey lime mudstone to fine to coarse-grained bioclastic wackestone and packstone with overturned and fragmented corals.	Development of isolated coralgal reef growth (patch reefs) in a warm, well-aerated shallow marine shelf (photic zone) with low to moderate energy level and normal salinity in general; the low-diversity coral framework suggests a stressed environment (Tucker and Wright, 1990).

and sandstone interbeds (F6, F7, and F12). The upper succession is composed of tabular, lenticular, and tabular cross-stratified conglomerates (F3, F4, and F7) with locally developed coral-algal reef and sandstone and mudstone interbeds (F14 and F15). The Kargı deposits initially appear to have been formed as a shallow braided stream and overbank deposit that developed on a medial alluvial fan. The upper succession with patch reefs indicates a sharp transgression over the alluvial fan, which in turn led to the development of a FD (Figure 6a).

Isolated piles of patch reefs bearing shallow-marine units are observed within the Kargı FD deposits (Figure 6b). The corals are characterized by generally columnar-shaped, thick-bedded, vertically growing *Porites* and *Tarbellastraea* colonies (Figure 6c). The age of this unit is attributed to the Tortonian based on corals such as

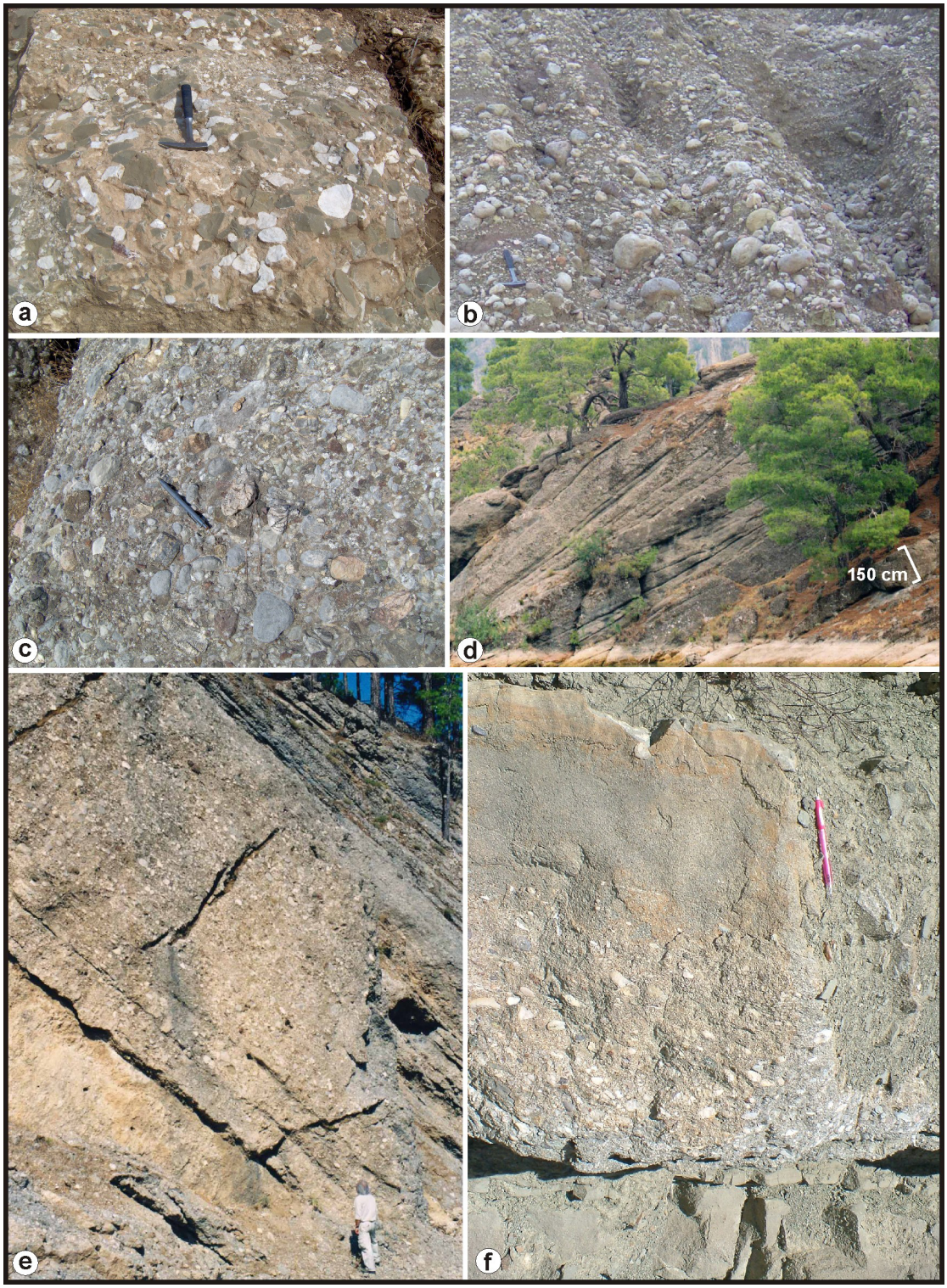

Figure 4. a) Limestone breccia (F1), b) matrix-supported conglomerate (F2), c) clast-supported conglomerate (F3), d) large-scale cross-stratified conglomerate (F4), e) parallel-stratified conglomerate (F5), f) graded conglomerate (F6), g) massive to parallel-stratified gravelly sandstone (F7), h) cross-stratified conglomerate and sandstone (F8), j) normally graded sandstone (F9), k) massive pebbly mudstone (F10), m) graded siltstone and mudstone (F11), n) massive to parallel laminated siltstone-mudstone (F12), p) chaotically folded deposits (F13), q) reefal debrites (F14), r) massive coral-algal boundstone (F15).

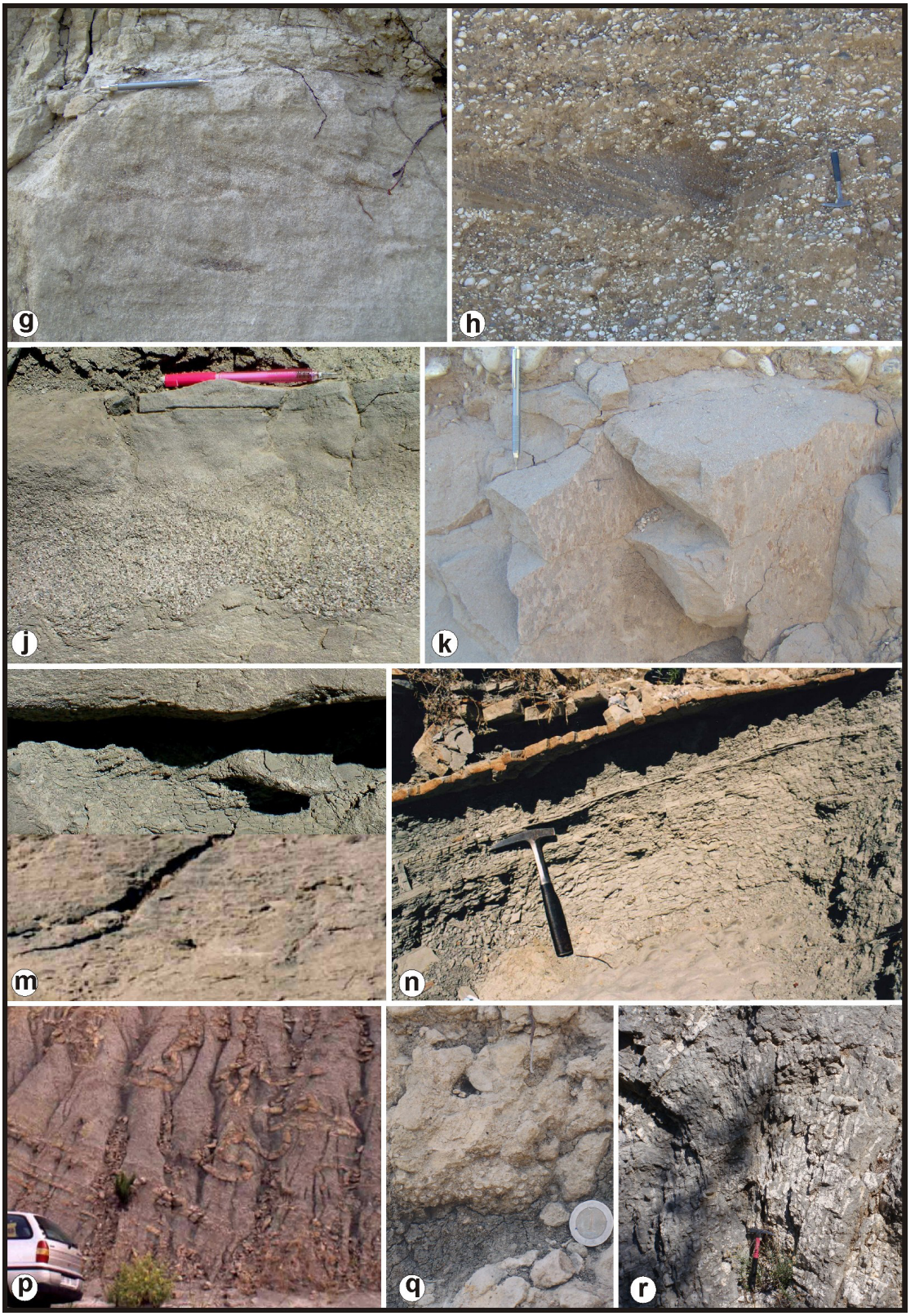

Figure 4. (Continued).

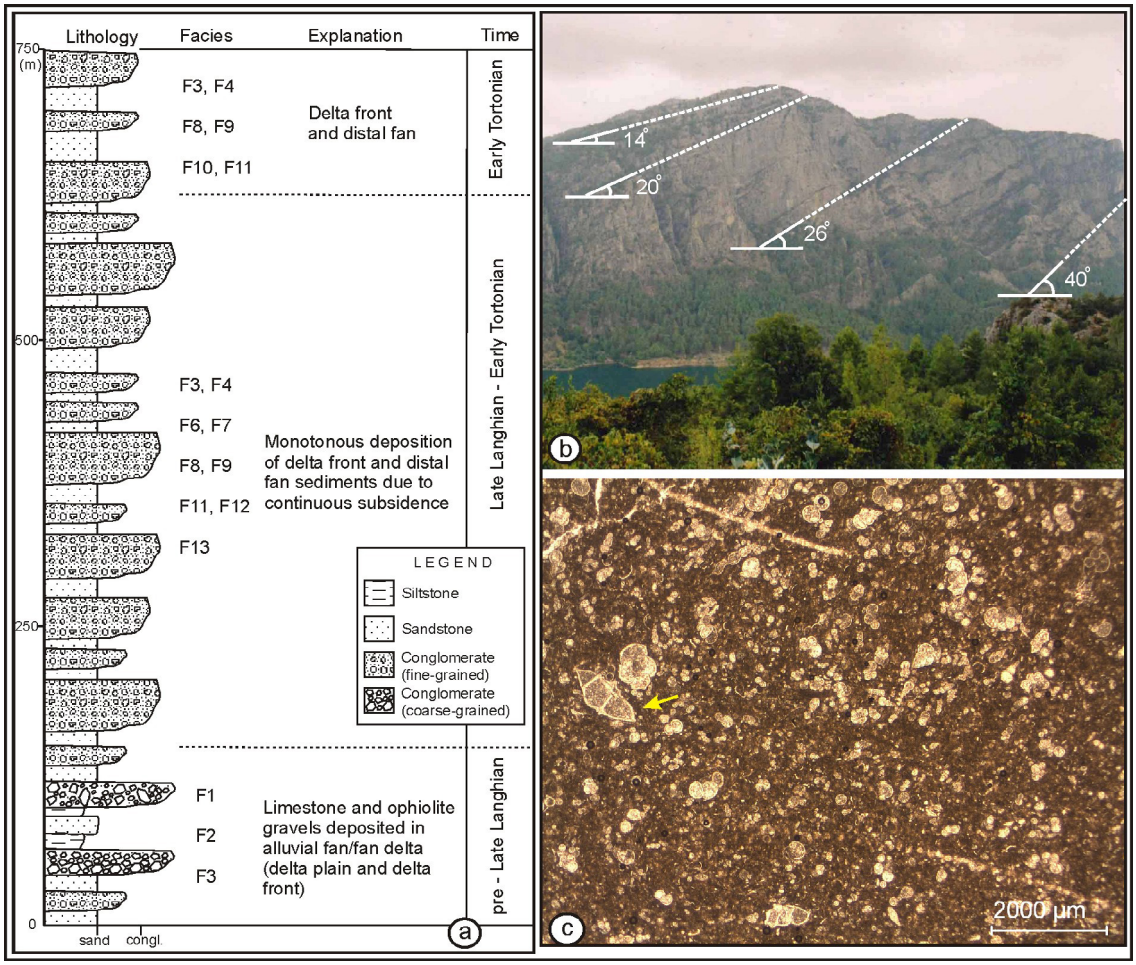

Figure 5. a) Measured stratigraphic section showing lithofacies and depositional subenvironments of the Karadağ FD deposits. b) Upward inclination decrease of bedding planes of the Karadağ FD deposits due to gradational subsidence. c) Upper Cretaceous Globotruncana determined in the Karadağ FD pebbles.

Porites lobatosepta and *Tarbellastraea siciliae* (Tuzcu and Karabıyıkoğlu, 2001; Karabıyıkoğlu et al., 2005). Patch reefs observed on FD deposits are composed of reef-core and back-reef units. While dendritic colonial corals characterize reef-core, coral fragments bounded by terrestrial-originated, red, coarse sandy matrix represent back-reef.

Field observations and petrographic studies indicate that the Bey Dağları Platform Carbonates and Antalya Nappes, similar to the Karadağ FD, fed the Kargı FD (Figure 7). Cross-beddings and imbrications indicate N-NE-oriented growing of the FD, compatible with the ones determined by Flecker et al. (1998).

7. Fan delta development and basin evolution

The tectonic phases mentioned above, which prevailed since the Langhian, have important roles for understanding the sedimentological evolution of the Aksu Basin.

7.1. Pre-Late Langhian period

The Aksu Basin is interpreted as a foreland basin (Flecker et al., 1998; Glover and Robertson, 1998a, 1998b). The formation and initial deformation of the basin is a consequence of the NW-SE-oriented contraction and southeastward movement of the Lycian Nappes. Shallow-marine deposits of the Karpuzçay Formation and the Karadağ FD of the Aksu Formation composed of clastics derived from the Bey Dağları Platform Carbonates and Antalya Nappes located to the western part of the area constitute the basin fill (Figure 8a). Paleocurrent measurements from imbrication and cross-bedding in the Karadağ FD deposits indicate that paleoflow direction was primarily towards the northeast (landward). This unusual progress of the Karadağ FD is associated with a deep depocenter situated on the landward side of the basin. This was accepted as evidence of foreland basin evolution for the Aksu Basin (Flecker et al., 1998). NE-SW-oriented

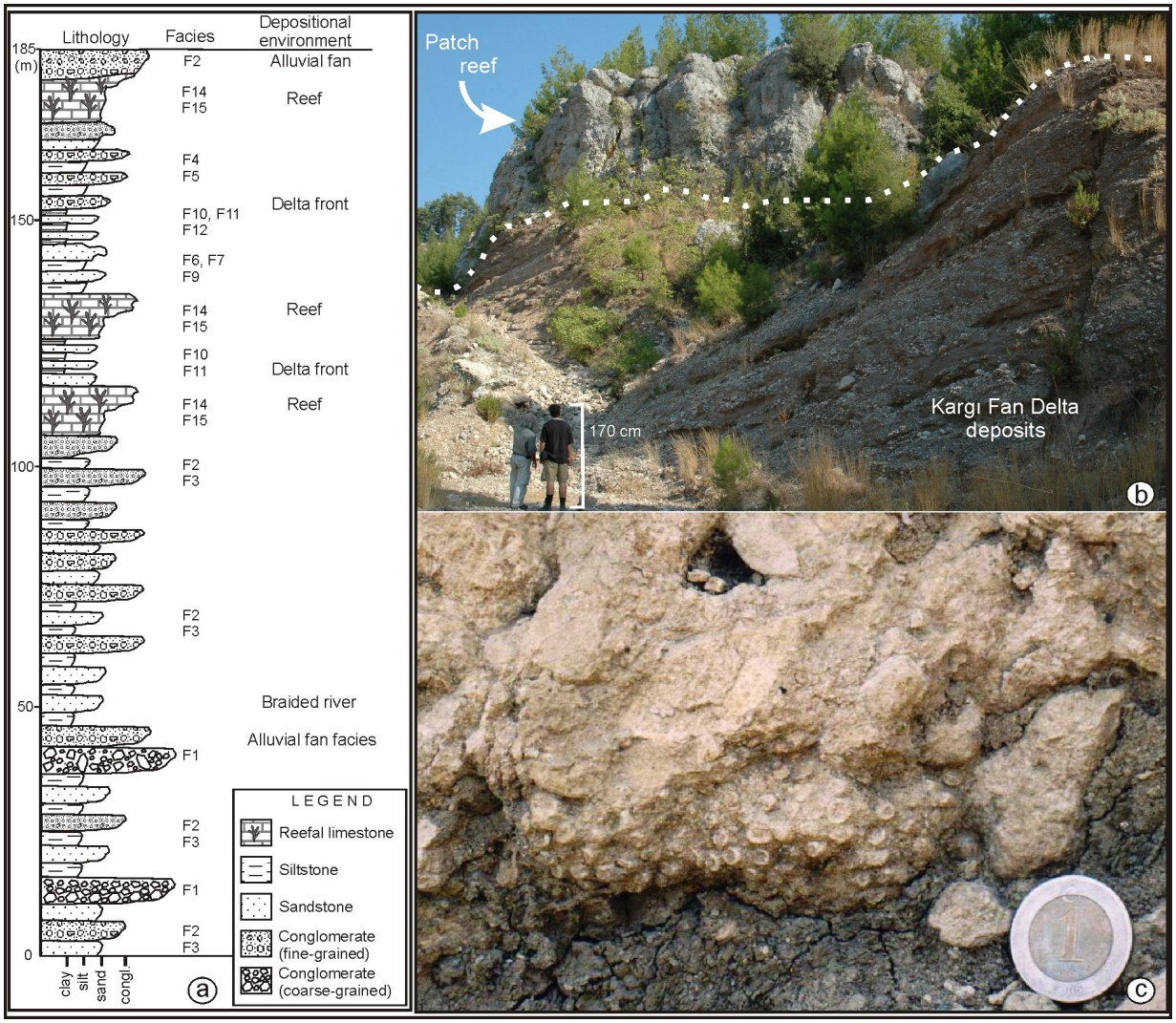

Figure 6. a) Measured stratigraphic section showing lithofacies and depositional subenvironments of the Kargı FD deposits. b) Patch reefs observed within the Kargı FD sediments (from Üner et al., 2011). c) Close-up view of the reef core facies with branching *Porites* colonies.

reverse faults observed at the lower levels of the Karadağ FD deposits were formed in the pre-Late Langhian period. This compressional regime was terminated by the emplacement of the Lycian Nappes at the end of the Langhian (Gutnic et al., 1979; Hayward, 1984; Poisson et al., 2003).

7.2. Late Langhian-Late Messinian period

A NW-SE-oriented tensional stress regime took place after the emplacement of the Lycian Nappes by the end of the Langhian. The development of the Karadağ FD continued under the control of this extension. Upward decrease in the inclination of thick conglomeratic layers clearly shows the gradual subsidence of the basin (Figure 5b).

The Tortonian Kargı FD is located between the Bey Dağları Platform Carbonates and the Karadağ FD. This situation shows that an accommodation space (approximately N-S trending) was created by the separation of the Karadağ FD from the Bey Dağları Carbonate Platform. Because of the extension during the Tortonian, this space was filled by Kargı FD deposits. The synsedimentary normal faults clearly indicate the ongoing extension during deposition of the Kargı FD. The Kapıkaya FD to the north and the Kozan FD and the Bucak FD to the east were deposited in the Langhian-Messinian period (Figure 8b).

The evolution of the FDs was terminated by the major regression period (5.6 Ma ago) of the Messinian Crisis (Hsü et al., 1973; Clauzon et al., 1996; Krijgsman et al., 1999; Rouchy and Caruso, 2006), the large-scale sea-level drop, rapid erosion, and desiccation that dominated

Figure 7. The positions of the Kargı and Karadağ FDs and the source area (Bey Dağları Platform Carbonates).

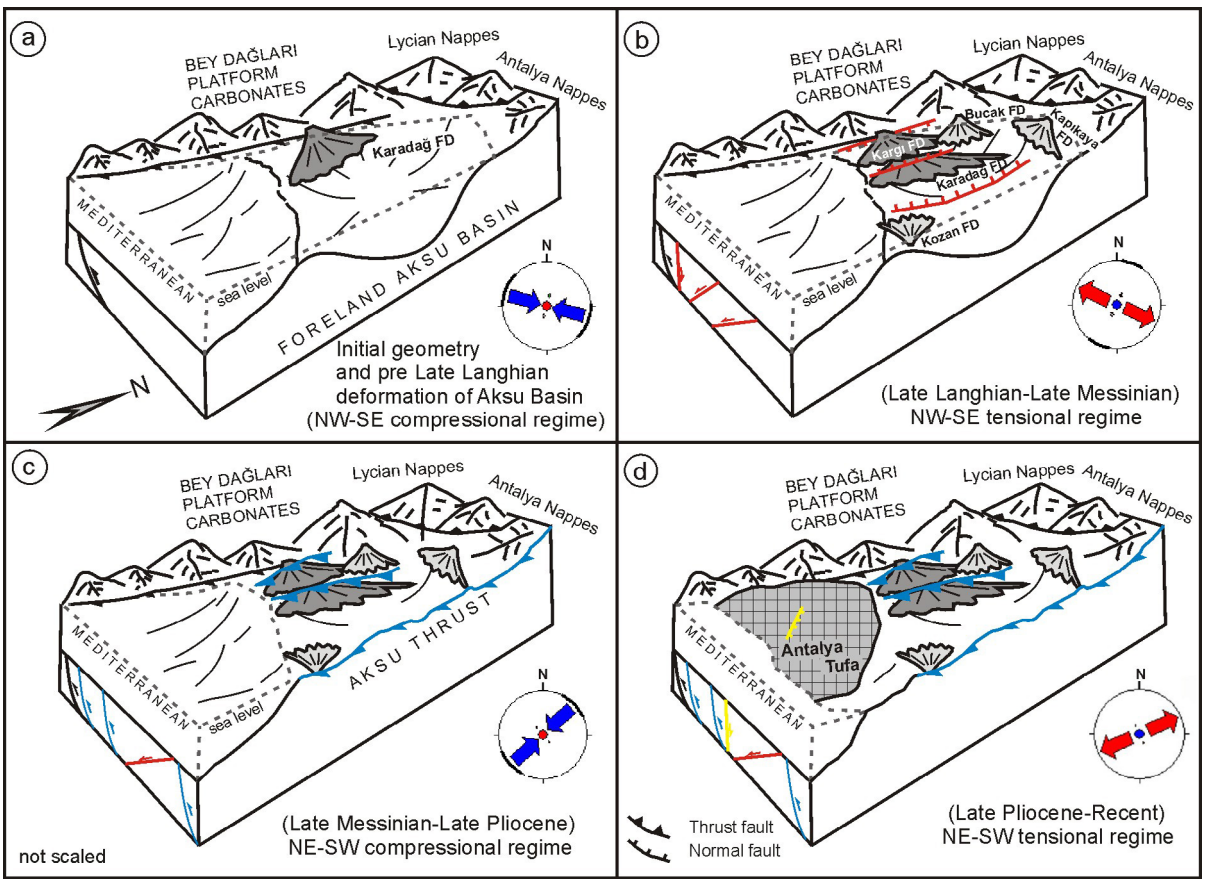

Figure 8. Geological evolution of the fan deltas in the Aksu Basin. a) Initial geometry of Aksu Basin and the development of the Karadağ FD under the control of NW-SE compressional regime. b) Formation of Kargı, Kapıkaya, Bucak, and Kozan FDs in NW-SE tensional regime. c) NE-SW compressional regime (Aksu Phase) faults and the new sea level after the Messinian Crisis. d) NE-SW tensional regime for the basin (Late Pliocene to Recent).

the Mediterranean region. This event also gave rise to the development of terrestrial conditions over marine depositional environments.

7.3. Late Messinian-Late Pliocene

The tensional stress regime that prevailed since the Late Langhian was replaced by a NE-SW-oriented compressional regime known as the Aksu Phase. This period is the erosional and deformational time interval of the FDs. By the increase of sea level in the Zanclean, marine conditions prevailed in the southern part of the basin while the northern part remained terrestrial (Figure 8c). Reefal limestones (Gebiz Limestones), alluvial FDs (Eskiköy Formation), and shallow-marine siltstone-marl alternations (Yenimahalle Formation) were deposited along the deep valleys incised during the "Messinian Crisis" sea-level drop (Figure 9). The Aksu Phase is known to have prevailed until the Late Pliocene (Poisson et al., 2003).

7.4. Late Pliocene-Recent

In the Late Pliocene, marine conditions disappeared, creating terrestrial environments in the Aksu Basin. Widespread lacustrine travertines and tufas were deposited in different parts of the basin during this period (Figure 8d). A compressional stress regime is superseded by a NE-SW-oriented tensional stress regime. This extension is characterized by normal faulting observed in lacustrine travertines and older units (Üner et al., 2015). GPS measurements and focal mechanism solutions of recent earthquakes support the ongoing extension in the Aksu Basin and surrounding region (McClusky et al., 2000).

8. Discussion

8.1. Basin formation

Three different models were suggested for the evolution of the Aksu Basin. These are (1) the basin's being evolved as a foreland basin due to the contraction generated by the emplacement of the Lycian Nappes (Flecker et al., 1998; Glover and Robertson, 1998a, 1998b; Robertson, 2000), (2) the depression's being far from the domain of the Lycian Nappes and formed as half-graben (Flecker et al., 2005), and (3) division of the postorogenic Antalya basin into three subbasins, namely the Aksu, Köprüçay, and Manavgat, due to the tensional and compressional stress in the Late Miocene (Karabıyıkoğlu et al., 2005).

The paleocurrent data obtained from the Karadağ and Kargı FDs (Figure 2b), the northward-developed Karadağ FD (against open sea), and the curved basin morphology support the foreland basin model. As the first tectonic phase, obtained from the paleostress analysis of Üner et al. (2015) and this study, is determined as a compressional stress regime, our model is not compatible with the half-graben model. The Middle-Late Miocene Karadağ, Kargı, Bucak, Kozan, and Kapıkaya FDs deposited at the margins of the Aksu Basin show that the basin already had the basin morphology before the Late Miocene tectonism. Because of this situation our study is not harmonious with the basin division model.

8.2. Miocene paleogeography of Aksu and adjacent basins

There are several Miocene basins located at the southern part of Anatolia (Adana, Mut, Manavgat, Köprüçay, Aksu, Çatallar, and Kasaba basins) (Figure 1a). These basins, mostly formed in the Early Miocene, slightly differ from each other with their paleogeographical evolution. FD formation and thick conglomeratic sequences of the Burdigalian-Langhian period are common at the margins of all basins except the Adana basin, the one located at the easternmost part of all depressions (Karabıyıkoğlu et al., 2004). The Adana basin experienced a rapid regression followed by the domination of a terrestrial environment while the remaining basins were controlled by shallow-marine conditions (Faranda et al., 2013; Ilgar et al., 2013). This regression is associated with the regional uplift caused by the Bitlis-Zagros Suture Zone where Arabian–Eurasian collision took place (Faranda et al., 2013). The Aksu and other basins, located far from this collision, were not affected by this event. Contrarily, the Serravalian-Tortonian period refers to thick FD sequence deposition (Karadağ FD) under shallow-marine conditions.

The main reason for the Miocene basins' (located at the Mediterranean coast of Turkey) deformation variety is the location of the Anatolian plate. The Adana Basin is shaped by the Cyprian arc and East Anatolian and Dead Sea Fault Systems while the Köprüçay and Manavgat basins are deformed by only the Cyprian arc. The Aksu, Çatallar, and Kasaba basins are dominated by both the Aegean and Cyprian arcs. Similar deformational characteristics on FDs are observed on other Mediterranean basins such as the Padan foreland basin (Italy) (Rossi and Rogledi, 1988), Almanzora Basin (Spain) (Darbio and Polo, 1988), and Ebro Basin (Spain) (Marzo and Anadón, 1988).

Although these basins are located at the northern part of the subduction zone, the timing of the related extension in these depressions differs from each other. This difference is associated with the retreat of the oceanic lithosphere (Glover and Robertson, 1998a; Kelling et al., 2005). As the location of the Aksu Basin is close to the junction point of the two arcs (Aegean and Cyprian arcs), it is possible to observe the deformational clues of each arc in the basin. The alternating compressional and tensional stress regimes obtained from paleostress analysis are thought to have generated from the activity of the arcs.

9. Conclusions

The Aksu Basin constitutes one of the important archives for temporal and spatial changes produced by the African-

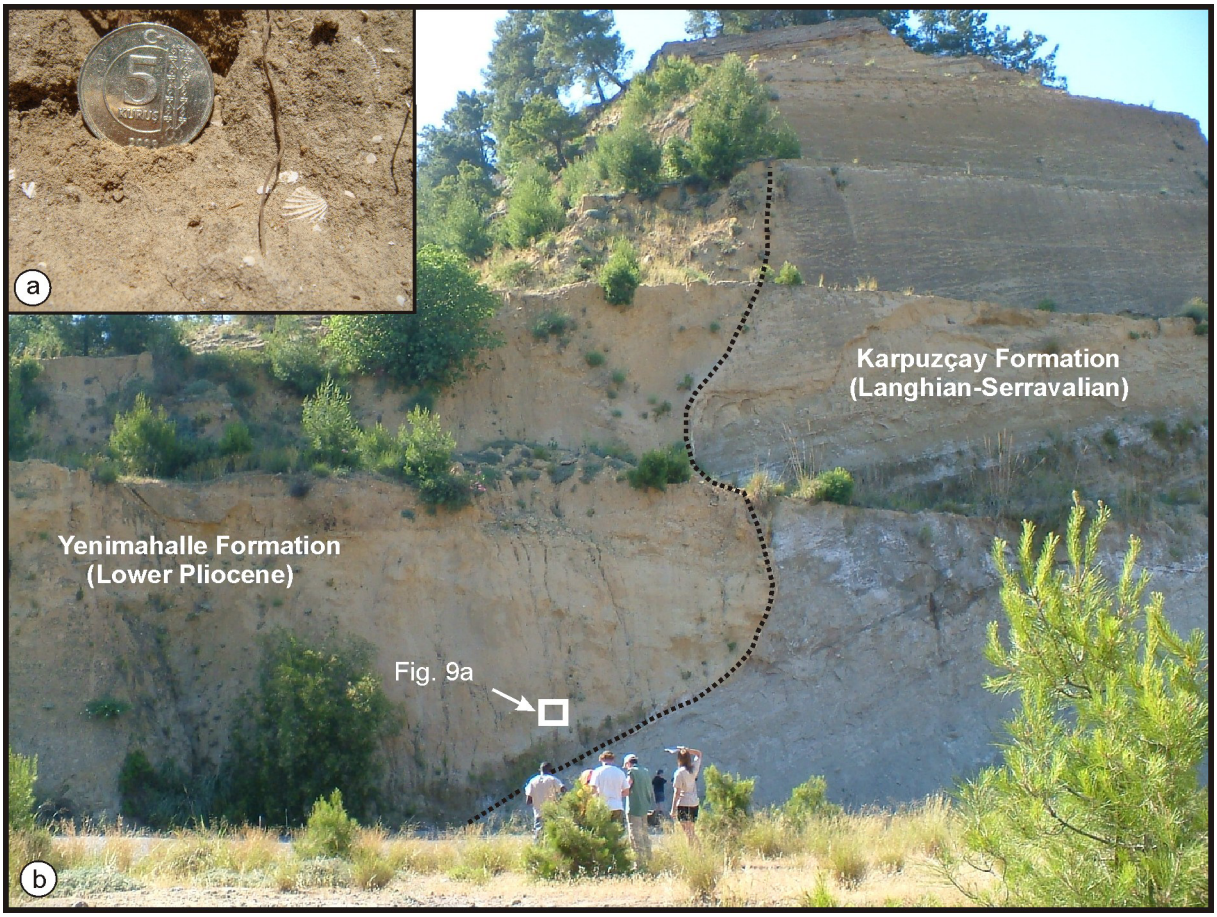

Figure 9. Incised valley eroded during the Messinian Crisis and the Pliocene infill. a) Close-up view of the Pliocene Yenimahalle Formation. b) General position of the incised valley.

Eurasian contraction, which affected both basin geometry and depositional systems, since its formation. Structural and sedimentological data, collected from the basin fill and margins, indicate complex tectonic and sedimentological evolution from the Langhian to Recent.

Debris and/or mass flow-dominated deposits, which constitute the major part of the deposition in the Aksu Basin, represent typical FD properties with their alluvial feeding systems, transitive deposits between terrestrial and shallow-marine conditions, and juxtaposing high-relief topography. The Karadağ, Kargı, and Bucak FDs to the west; the Kozan FD to the east; and the Kapıkaya FD to the north of the basin are major examples.

FDs provide important records about the geological evolution of the Aksu Basin. The Karadağ and Kargı FDs were strongly affected by the tectonism in the basin. The NW-SE-oriented tensional stress regime, which prevailed during the Langhian-Messinian period, separated the Karadağ FD from its origin/source. This accommodation space was later filled with the Kargı FD deposits.

The shallow FD fronts were affected by sea level changes and climatic factors. The patch-reefs observed in the Karadağ and Kargı FDs point toward a deposition that occurred during the decrease/pause in the terrestrial clastic input and interruption of FD development, which were both due to the sudden increase of sea level. The existence of reefal limestones (as an indicator of a transgressive period) in FD deposits gives information about the climatic and environmental conditions that prevailed during the FD development. *Porites*- and *Tarbellastraea*-rich reefs are the major indicators of the FD development at medium-high wave energy-dominated shore under the control of a temperate to tropic-subtropic climate.

There are several differences between the Aksu and adjacent basins in terms of deposition processes and paleogeographical evolution. The depositional and erosional periods of these basins vary, especially after the Messinian Crisis. The main reason for this variety is the evolution of these basins under different tectonic processes and structures. This study demonstrates that

an understanding of spatial and temporal distributions of FDs under the control of tectonic instability is crucial for the reconstruction of the basin geometry, architecture of the FDs, and dynamics of the depositional history.

Acknowledgments
This study was financially supported by a Hacettepe University Scientific Research Project (BAB-05D09602001). We also appreciate Kevin McClain for English editing.

References

Akay E, Uysal Ş (1984). Orta Torosların batısındaki (Antalya) Neojen Çökellerinin Stratigrafisi, Sedimantolojisi ve Yapısal Jeolojisi. MTA Raporu No: 2147. Ankara, Turkey: MTA (in Turkish).

Akay E, Uysal Ş, Poisson A, Cravatte J, Müller C (1985). Stratigraphy of the Antalya Neogene Basin. Türkiye Jeoloji Kurumu Bülteni 28: 105-119 (in Turkish with an abstract in English).

Barka AA, Reilinger R, Şaroğlu F, Şengör AMC (1997). The Isparta Angle: its importance in the neotectonics of the Eastern Mediterranean Region. In: Pişkin O, Ergün M, Savaşçın MY, Tarcan G, editor. Proceedings of International Earth Sciences Colloquium on the Aegean Region. İzmir, Turkey: Dokuz Eylül University, pp. 3-18.

Blirka LH, Nemec W (1998). Postglacial colluvium in western Norway: depositional processes, facies and paleoclimatic record. Sedimentology 45: 909-959.

Blumenthal MM (1951). Recherces géologiques dans le Taurus occidental dans l'arrière-pays d'Alanya. Mineral Research and Exploration Institute of Turkey (MTA) Publications, Series D5. Ankara, Turkey: MTA (in French).

Bouma A (1962). Sedimentology of Some Flysch Deposits. A Graphic Approach to Facies Interpretation. Amsterdam, the Netherlands: Elsevier.

Çiner A, Doğan U, Yıldırım C, Akçar N, Ivy-Ochs S, Alfimov V, Kubik PW, Schlüchter C (2015). Quaternary uplift rates of the Central Anatolian Plateau, Turkey: Insights from cosmogenic isochron-burial nuclide dating of the Kızılırmak River terraces. Qua Sci Rev 107: 81-97.

Çiner A, Karabıyıkoğlu M, Monod O, Deynoux M, Tuzcu S (2008). Late Cenozoic sedimentary evolution of the Antalya basin, southern Turkey. Turkish J Earth Sci 17: 1-41.

Clauzon G, Suc JP, Gautier F, Berger A Loutre MF (1996). Alternate interpretation of the Messinian salinity crisis: controversy resolved? Geology 24: 363-366.

Cook HE, Mullins HT (1983). Basin margin environment. In: Scholle PA, Bebout DG, Moore CH, editors. Carbonate Depositional Environments. Tulsa, OK, USA: American Association of Petroleum Geologists, pp. 540-617.

Darbio CJ, Polo MD (1988). Late Neogene fan deltas and associated coral reefs in the Almanzora Basin, Almeria Province, southern Spain. In: Nemec W, Steel RJ, editors. Fan Deltas: Sedimentology and Tectonic Setting. London, UK: Blackie and Son, pp. 354-367.

Deynoux M, Çiner A, Monod O, Karabıyıkoğlu M, Manatschal G, Tuzcu S (2005). Facies architecture and depositional evolution of alluvial fan to fan-delta complexes in the tectonically active Miocene Köprüçay Basin, Isparta Angle, Turkey. Sedim Geol 173: 315-343.

Dumont JF, Kerey E (1975). Basic geological study of southern lake of Eğirdir. Türkiye Jeoloji Kurumu Bülteni 18: 169-174 (in Turkish with an abstract in English).

Faranda C, Gliozzi E, Cipollar P, Grossi F, Darbaş G, Gürbüz K, Nazik A, Gennari R, Cosentino D (2013). Messinian paleoenvironmental changes in the easternmost Mediterranean Basin: Adana Basin, southern Turkey. Turkish J Earth Sci 22: 839-863.

Flecker R, Ellam RM, Müller C, Poisson A, Robertson AHF, Turner J (1998). Application of Sr isotope stratigraphy and sedimentary analysis to the origin and evolution of the Neogene basins in the Isparta Angle, southern Turkey. Tectonophysics 298: 83-101.

Flecker R, Poisson A, Robertson AHF (2005). Facies and palaeogeographic evidence for the Miocene evolution of the Isparta Angle in its regional eastern Mediterranean context. Sedim Geol 173: 277-314.

Glover CP, Robertson AHF (1998a). Neotectonic intersection of the Aegean and Cyprus tectonic arcs: extensional and strike-slip faulting in the Isparta Angle, SW Turkey. Tectonophysics 298: 103-132.

Glover CP, Robertson AHF (1998b). Role of regional extension and uplift in the Plio-Pleistocene evolution of the Aksu Basin, SW Turkey. J Geol Soci 155: 365-387.

Gutnic M, Monod O, Poisson A, Dumont JF (1979). Géologie des Taurides occidentales (Turquie). Mémoire de la Societé Géologique de France 137: 1-112 (in French).

Hall J, Aksu AE, King H, Gogacz A, Yaltırak C, Çiftçi G (2014). Miocene–Recent evolution of the western Antalya Basin and its linkage with the Isparta Angle, eastern Mediterranean. Marine Geol 349: 1-23.

Hayward AB (1984). Miocene clastic sedimentation related to the emplacement of the Lycian Nappes and the Antalya Complex. Geol Soc Sp 17: 287-300.

Hayward AB, Robertson AHF (1982). Direction of ophiolite emplacement inferred from Cretaceous and Tertiary sediments of an adjacent autochthon, the Bey Dağlari, southwest Turkey. GSA Bulletin 93: 68-75.

Hsü KJ, Ryan WBF, Cita MB (1973). Late Miocene desiccation of the Mediterranean. Nature 242: 240-244.

Ilgar A, Nemec W, Hakyemez A, Karakuş E (2013). Messinian forced regressions in the Adana Basin: a near-coincidence of tectonic and eustatic forcing. Turkish J Earth Sci 22: 864-889.

Karabıyıkoğlu M, Çiner A, Deynoux M, Monod O, Tuzcu S, Manatschal G (2004). Miocene Tectono-sedimentary Evolution of the Late Cenozoic Antalya Basin. MTA-CNRS (France)-TÜBİTAK Co-Project. Ankara, Turkey: TÜBİTAK.

Karabıyıkoğlu M, Çiner A, Monod O, Deynoux M, Tuzcu S, Örçen S (2000). Tectono-sedimentary evolution of the Miocene Manavgat Basin, Western Taurids, Turkey. Geol Soc Sp 173: 271-294.

Karabıyıkoğlu M, Tuzcu S, Çiner A, Deynoux M, Örçen S, Hakyemez A (2005). Facies and environmental setting of the Miocene coral reefs in the Late-Orogenic fill of the Antalya Basin, western Taurides, Turkey: implications for tectonic control and sea level changes. Sedim Geol 173: 345-371.

Kelling G, Robertson AHF, Buchem FV (2005). Cenozoic sedimentary basins of southern Turkey: an introduction. Sedim Geol 173: 1-13.

Koç A, van Hinsbergen DJJ, Kaymakçı N, Langereis CG (2016). Late Neogene oroclinal bending in the central Taurides: a record of terminal eastward subduction in southern Turkey? Earth Planet Sc Lett 434: 75-90.

Koçyiğit A, Özacar AA (2003). Extensional neotectonic regime through the NE edge of outer Isparta Angle, SW Turkey: new field and seismic data. Turkish J Earth Sci 12: 67-90.

Koşun E (2012). Facies characteristics and depositional environments of Quaternary tufa deposits, Antalya, SW Turkey. Carbonate Evaporite 27: 269-289.

Koşun E, Poisson A, Çiner A, Wernli R, Monod O (2009). Syn-tectonic sedimentary evolution of the Miocene Çatallar basin, southwestern Turkey. J Asian Earth Sci 34: 466-479.

Krijgsman W, Hilgen FJ, Raffi I, Sierro FJ, Wilson DS (1999). Chronology, causes and progression of the Messinian salinity crisis. Nature 400: 652-655.

Lowe DR (1982). Sediment gravity flows: depositional models with special reference to the deposits of high density turbidity currents. J Sedim Petr 52: 279-297.

Marzo M, Anadón P (1988). Anatomy of a conglomeratic fan-delta complex: the Eocene Montserrat Conglomerate, Ebro Basin, northeastern Spain. In: Nemec W, Steel RJ, editors. Fan Deltas: Sedimentology and Tectonic Setting. London, UK: Blackie and Son, pp. 318-340.

Massari F, Parea GC (1988). Progradational gravel beach sequences in a moderate to high energy, microtidal marine environment. Sedimentology 35: 881-913.

McClusky S, Balassanian S, Barka A, Demir C, Ergintav S, Georgiev I, Gurkan O, Hamburger M, Hurst K, Kahle H et al. (2000). Global positioning system constraints on plate kinematics and dynamics in the Eastern Mediterranean and Caucasus. J Geophy Res 105: 5695-5719.

McPerson JG, Shanmugam G, Moiola RJ (1987). Fan-deltas and braid deltas: varieties of coarse-grained deltas. GSA Bulletin 99: 331-340.

Middleton GV, Hampton MA (1976). Subaqueous sediment transport and deposition by sediment gravity flows. In: Stanley DJ, Swift DJP, editors. Marine Sediment Transport and Environmental Management. New York, NY, USA: Wiley, pp. 197-218.

Monod O, Kuzucuoğlu C, Okay Aİ (2006). A Miocene Palaeovalley Network in the Western Taurus (Turkey). Turkish J Earth Sci 15: 1-23.

Nemec W, Steel RJ (1988). What is a fan delta and how do we recognize it? In: Nemec W, Steel RJ, editors. Fan Deltas: Sedimentology and Tectonic Setting. London, UK: Blackie and Son, pp. 3-13.

Orton GJ (1988). A spectrum of Middle Ordovician fan deltas and braidplain deltas, North Wales: a consequence of varying fluvial clastic input. In: Nemec W, Steel RJ, editors. Fan Deltas: Sedimentology and Tectonic Setting. London, UK: Blackie and Son, pp. 23-49.

Özsayın E (2007). Neogene–Quaternary structural evolution of İnönü–Eskişehir Fault System between Yeniceoba–Cihanbeyli (Konya–Turkey). PhD, Hacettepe University, Ankara, Turkey (in Turkish with an abstract in English).

Özsayın E, Çiner TA, Rojay FB, Dirik RK, Melnick D, Fernandez-Blanco D, Bertotti G, Schildgen TF, Garcin Y, Strecker MR et al. (2013). Plio-Quaternary extensional tectonics of the Central Anatolian Plateau: a case study from the Tuz Gölü Basin, Turkey. Turkish J Earth Sci 22: 691-714.

Özsayın E, Dirik K (2007). Quaternary activity of the Cihanbeyli and Yeniceoba fault zones: İnönü-Eskişehir Fault System, Central Anatolia. Turkish J Earth Sci 16: 471-492.

Özsayın E, Dirik K (2011). The role of oroclinal bending in the structural evolution of the Central Anatolian Plateau: evidence of a regional changeover from shortening to extension. Geol Carpath 62: 345-359.

Pickering KT, Stow DAV, Watson M, Hiscott RN (1986). Deepwater facies, processes and models: a review and classification scheme for modern and ancient sediments. Earth Sci Rev 22: 75-174.

Poisson A, Orszag-Sperber F, Koşun E, Bassetti MA, Müller C, Wernli R, Rouchy JM (2011). The Late Cenozoic evolution of the Aksu basin (Isparta Angle; SW Turkey): new insights. Bulletin Société Géologique de France 182: 133-148.

Poisson A, Wernli R, Sağular EK, Temiz H (2003). New data concerning the age of the Aksu Thrust in the south of the Aksu valley, Isparta Angle (SW Turkey): consequences for the Antalya Basin and the Eastern Mediterranean. Geol J 38: 311-327.

Postma G, Babic L, Zupanic J, Roe SL (1988). Delta-front failure and associated bottomset deformation in a marine, gravelly Gilbert-type fan delta. In: Nemec W, Steel RJ, editors. Fan Deltas: Sedimentology and Tectonic Setting. London, UK: Blackie and Son, pp. 91-102.

Robertson AHF (2000). Mesozoic-Tertiary tectonic-sedimentary evolution of a south Tethyan oceanic basin and its margins in southern Turkey. Geol Soc Sp 173: 97-138.

Rossi ME, Rogledi S (1988). Relative sea-level changes, local tectonic settings and basin margin sedimentation in the interference zone between two orogenic belts: seismic stratigraphic examples from the Padan foreland basin, northern Italy. In: Nemec W, Steel RJ, editors. Fan Deltas: Sedimentology and Tectonic Setting. London, UK: Blackie and Son, pp. 368-384.

Rouchy JM, Caruso A (2006). The Messinian salinity crisis in the Mediterranean Basin: a reassessment of the data and an integrated scenario. Sedim Geol 188: 35-67.

Schildgen TF, Cosentino D, Caruso A, Buchwaldt R, Yıldırım C, Rojay B, Bowring SA, Echtler H, Strecker MR (2012). Surface expression of Eastern Mediterranean slab dynamics: Neogene topographic and structural evolution of the SW margin of the Central Anatolian Plateau, Turkey. Tectonics 31: 1-21.

Şenel M (1997). 1:250 000 ölçekli Türkiye Jeoloji Haritaları, No. 4, Isparta Paftası. Ankara, Turkey: MTA Genel Müdürlüğü Jeoloji Etütleri Dairesi (in Turkish).

Tucker ME, Wright VP (1990). Carbonate Sedimentology. Oxford, UK: Blackwell Scientific.

Tuzcu S, Karabıyıkoğlu M (2001). Batı Toros Kuşağı Miyosen Mercan Resiflerinin Paleontolojisi, Stratigrafisi, Fasiyesleri ve Çökelme Ortamları, MTA Genel Müdürlüğü, Jeoloji Etütleri Dairesi, Rapor No: 10438. Ankara, Turkey: MTA (in Turkish).

Üner S (2009). Geological evolution of the Aksu (Antalya) Miocene basin. PhD, Hacettepe University, Ankara, Turkey (in Turkish with an abstract in English).

Üner S, Dirik K, Çiner A (2011). Late Miocene Evolution of Kargı Fan Delta (Aksu Basin, Antalya). Yerbilimleri 32: 121-138 (in Turkish with an abstract in English).

Üner S, Özsayın E, Kutluay A, Dirik K (2015). Polyphase tectonic evolution of the Aksu Basin, Isparta Angle, southern Turkey. Geol Carpath 66: 157-169.

Zitter TAC, Woodside JM, Mascle J (2003). The Anaximander Mountains: a clue to the tectonics of southwest Anatolia. Geol J 38: 375-394.